Assessing Homopolymer Distribution in ABC Triblock Copolymer/ Homopolymer Blends through a Transition in Interfacial Geometry

R. L. Lescanec,*,†,‡ L. J. Fetters,§ and E. L. Thomas*,†

Department of Materials Science and Engineering, Massachusetts Institute of Technology, Cambridge, Massachusetts 02139, and Exxon Research and Engineering Company, Corporate Research Science Laboratory, Clinton Township, Annandale, New Jersey 08801

Received September 26, 1997; Revised Manuscript Received December 26, 1997

ABSTRACT: Intermaterial dividing surfaces (IMDS) in strongly segregated block copolymer systems are typically of constant mean curvature (CMC). This observation largely derives from the interplay of the thermodynamics of chain deformation and interfacial tension. Recently, a compositionally symmetric, linear poly(2-vinylpyridine)-*b*-polyisoprene-*b*-polystyrene (P2VP−PI−PS) triblock copolymer with each block having a $M_w \sim 15\,000$, was observed to order in a hexagonal lattice of P2VP cylinders, surrounded by a PI annulus within a PS matrix. The PI/PS IMDS was of non-CMC, assuming a pseudohexagonal cross section. This striking morphological behavior originates from the nonuniform degree of chain deformation occurring in the microstructure and indicates that the PI/PS IMDS is strongly coupled to the shape of the Wigner−Seitz cell of the microdomain lattice. We further probe this phenomenon by attempting to alter the curvature of the PI/PS interface through incorporation of homopolystyrene (h-PS) into the PS matrix by preparing P2VP−PI−PS/h-PS (PIS/S) blends having a composition of 90/10 (v/v) and $(M_w)_{h-PS} \sim 4000-100\,000$. Using TEM and SAXS, we observe a transition in the PI/PS IMDS as a function of the molecular weight of h-PS. When $(M_w)_{h-PS} < 50\,000$, the tethered PS blocks behave as "wet brushes". In this regime, the non-CMC character of the PI/PS IMDS is preserved and a slight contraction in the domain spacing is observed due to a nearly uniform distribution of h-PS in the matrix. When $(M_w)_{h-PS} = 50\,000$, behavior characteristic of the "dry brush" regime is seen. The PI/PS IMDS appears nearly circular in cross section with an accompanying increase in the domain spacing relative to that of the neat triblock. This behavior originates from a nonuniform distribution of h-PS in the matrix, with preferential segregation to the corners of the Wigner−Seitz cell. As the molecular weight of h-PS is further increased, the homopolymer is ejected from the microdomain structure and macrophase separates from the tethered PS blocks.

1. Introduction

Over the last few decades, an enormous amount of investigation, both experimental and theoretical, focused on elucidating the physics of phase morphology exhibited by block copolymer systems consisting of two distinct chemical species.[1−3] Elegant and precise synthetic techniques produced well-defined two-component block copolymers varying in architecture, molecular weight, and composition.[1,3] The equilibrium microstructures of these phase-separated materials vary markedly in symmetry. As part of the classification of a microdomain structure, the geometry of its intermaterial dividing surface (IMDS) is analyzed. Recently, considerable attention has focused on understanding the origin of complex microstructures having triply periodic IMDS.[1] Currently, the detailed nature of the curvature of the IMDS in these complex microstructures is under theoretical debate.[4,5] However, for the most part, the well-ordered classical microdomain geometries display IMDS having constant mean curvature (CMC), particularly in the strong segregation regime.[1,2]

A natural evolution of the synthetic protocols enabled the morphological study of block copolymers consisting of three distinct chemical components (ABC triblock copolymers).[6−16] Morphological characterization of several distinct ABC triblock copolymer systems has revealed a rich new set of well-ordered microdomain structures, several of which exhibit highly non-CMC IMDS.[12,15,16] The first example of a non-CMC microdomain structure was observed in microphase-separated, symmetric, linear poly(2-vinylpyridine)-*b*-polyisoprene-*b*-polystyrene (P2VP−PI−PS) triblock copolymers.[12] Transmission electron microscopy (TEM) studies of this material revealed hexagonally packed microdomains consisting of a P2VP core surrounded by a PI annulus within a PS matrix phase.[12] The most striking morphological feature clearly exhibited by this system was a PI/PS IMDS which appeared hexagonal in cross section.[12] This clear observation of a non-CMC IMDS existing in a microstructured block copolymer material is the motivation for the morphological study presented here.

The presence of both a non-CMC PI/PS IMDS and PI blocks exhibiting an azimuthally varying degree of deformation are energetically unfavorable. Therefore, we attempt to alter the shape of the IMDS (and the energetics of the triblock copolymer system) through the addition of homopolystyrene (h-PS) into the matrix phase. The dependence of the shape of the PI/PS IMDS on the molecular weight of h-PS is investigated at constant P2VP−PI−PS/h-PS (PIS/S) blend composition.

The remainder of this paper is organized as follows. After discussing our experimental procedure, we present the results of the TEM and SAXS characterization of the blends. We examine the effect of the molecular weight of h-PS component on the shape of the PI/PS IMDS. In our discussions, we account for the morpho-

† Massachusetts Institute of Technology.
‡ Present address: Corporate Research and Development Laboratories, The Gillette Company, Boston, MA 02127.
§ Exxon Research and Engineering Company.

S0024-9297(97)01426-5 CCC: $15.00 © 1998 American Chemical Society
Published on Web 02/18/1998

Table 1. P2VP−PI−PS Triblock Copolymer Molecular Characteristics

$(M_w)_{P2VP}$	$(M_w)_{PI}$	$(M_w)_{PS}$	$(M_w/M_n)_{PS}$	$(M_w/M_n)_{P2VP-PI-PS}$	ϕ_{P2VP}[a]	ϕ_{PI}[a,b]	ϕ_{PS}[a]
15 100	13 000	14 900	1.04	1.05	0.33	0.34	0.33

[a] Volume fraction of component in triblock copolymer. [b] Volume fraction of PI (70% *cis*-1,4, 24% *trans*-1,4, 6% 3,4) in triblock copolymer.

Table 2. Characteristics of P2VP−PI−PS/h-PS (PIS/S) Blends

sample	ϕ_{h-PS}[a]	$(M_w)_{h-PS}$	$(M_w/M_n)_{h-PS}$	ϕ_{P2VP}[b]	ϕ_{PI}[b]	ϕ_{PS}[b]
PIS/S-1	0.10	4 000	1.04	0.30	0.30	0.40
PIS/S-2	0.10	50 000	1.04	0.30	0.30	0.40

[a] Volume fraction of homopolystyrene in the blend. [b] Total volume fraction of component in the blend.

logical behavior observed in the PIS/S blends in terms of the distribution of h-PS in the matrix phase and its effect on the energetics describing the microphase-separated blends. We close by suggesting directions for further investigation of the PIS/S blends.

2. Experimental Section

The compositionally symmetric P2VP−PI−PS triblock copolymer was synthesized through sequential living anionic polymerization of styrene, 1,4-isoprene, and 2-vinylpyridine monomers using high-vacuum techniques.[17] Styrene monomer was polymerized in solution with benzene at 30 °C first using *sec*-butyllithium as the initiator. After polymerization, an aliquot of PSLi was removed for GPC analysis. 1,4-Isoprene monomer was then added to the reaction solution containing the living polystyryl anions. After the living PS−PILi solution was diluted with THF at a ∼2:1 ratio (THF/benzene), 2-vinylpyridine was then added. During this step the reaction vessel was immersed in a dry ice/2-propanol bath at −70 °C to minimize linking and branching side reactions involving the azomethane unit on the pyridine ring. Termination was done ∼30 min after the addition of the pyridine monomer.

Molecular weight distributions were determined for the PS block, the PS−PI diblock, and the entire triblock copolymer using a high-resolution (six linear Ultratyragel columns) Waters 150C gel permeation chromatograph calibrated with polystyrene and polyisoprene standards. The solvent was THF with ∼2 vol % of pyridine present. This was done to minimize absorption within the columns. In the absence of pyridine, the apparent M_w/M_n was 1.15, while with pyridine in the carrier solvent, the ratio was 1.05. The composition of the triblock copolymer was determined to an accuracy of ±1 mol % using a Bruker 400-MHz ^{1}H NMR spectrometer. The molecular characteristics of the compositionally symmetric P2VP−PI−PS triblock copolymer are shown in Table 1.

Five PIS/S blends were prepared by blending the neat triblock with nearly monodisperse h-PS having M_w = 4000, 9000, 23 000, 50 000, and 100 000 in a ratio of 90/10 (v/v). We will focus our discussion on blends in which the M_w of h-PS are 4000 and 50 000. The h-PS samples were obtained from Pressure Chemical Co. (Pittsburgh, PA) and were reprecipitated from a toluene solution, filtered, and dried before use. The molecular characteristics of h-PS and the two blend compositions on which we will center our morphological characterization are shown in Table 2.

Blend specimens for TEM and SAXS characterization were quiescently cast from solution with tetrahydrofuran (THF) (5% w/v) over a period of 5 days. The resulting films, approximately 1 mm thick, were then placed under vacuum at room temperature for 1 day to remove any residual solvent. In an effort to obtain near-equilibrium microstructures, the films were subsequently annealed above the T_g of the PS and P2VP components, at 120 °C for 1 week, under vacuum. We anticipate this protocol will yield microstructures with optimum long-range order.[1] Ultrathin sections (∼50 nm) for TEM characterization were obtained by cryomicrotomy using a Reichert-Jung FC4E microtome equipped with a diamond knife. To enhance mass−thickness contrast in the blends, the microtomed sections were stained with OsO_4 vapors. Bright-field TEM was performed on a JEOL 200CX transmission electron microscope having either a tungsten or LaB_6 filament operated at an accelerating voltage of 200 kV. SAXS was performed using Cu Kα X-rays from a Rigaku RU-200BH rotating-anode X-ray generator equipped with a 0.2 × 2 mm microfocus cathode and Franks mirror optics. Two-dimensional images were collected with an image-intensified area CCD detector.[18] After collection, the images were digitized and corrected for detector response characteristics. Domain spacings were calculated from one-dimensional intensity profiles obtained by integrating the two-dimensional patterns azimuthally along an arc ±15° from the axis normal to the polymer film surface.

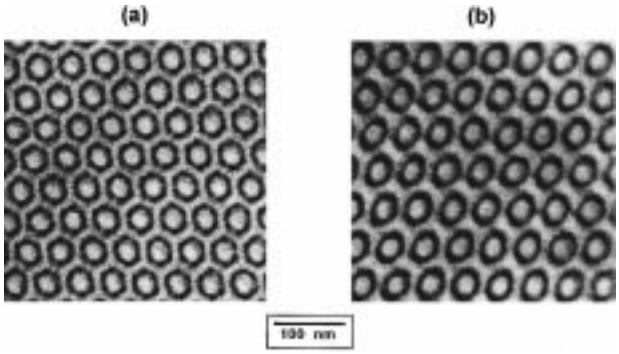

Figure 1. Bright-field TEM micrographs of PIS/S-1 (a) and PIS/S-2 (b). Nearly axial projections of hexagonally ordered microdomains consisting of a P2VP core surrounded by a PI annulus (dark due to OsO_4 staining) in a PS matrix are observed.

3. Results and Discussion

To ensure that the non-CMC morphology observed in the neat triblock copolymer was not an artifact of the solution casting procedure,[1] attempts were made to cast the P2VP−PI−PS copolymer from toluene (slightly preferential for PS: $\delta_{PS} = 9.1$ (cal/cm^3)$^{1/2}$, $\delta_{tol} = 8.9$ (cal/cm^3)$^{1/2}$), cyclohexane (preferential for PI: $\delta_{PI} = 8.2$ (cal/cm^3)$^{1/2}$, $\delta_{c-hex} = 8.2$ (cal/cm^3)$^{1/2}$), and pyridine (preferential for P2VP: $\delta_{P2VP} = 10.0$ (cal/cm^3)$^{1/2}$, $\delta_{pyr} = 10.7$ (cal/cm^3)$^{1/2}$)).[19] Optically clear films were obtained from films cast from toluene, and pyridine, as well as THF. The triblock was insoluble in cyclohexane, presumably due to the large difference between δ_{c-hex} and δ_{P2VP}, since PS−PI diblocks are soluble in cyclohexane and toluene. After annealing each sample according to the protocol stated above, bright-field TEM was performed. The non-CMC morphology described previously[12] was observed in each film when examined by TEM, indicating that the choice of solvent has little effect on the symmetry of the morphology of the microphase-separated triblock copolymer. We therefore conclude that the microstructure exhibited by the neat triblock is at thermodynamic equilibrium and is not an artifact of the casting procedure. The sample cast from THF exhibited the largest grain structure; therefore, THF was selected as the solvent for the blend preparation.

Parts a and b of Figure 1 show bright-field TEM images of OsO_4-stained PIS/S-1 and PIS/S-2, respectively. Prior investigation of the neat triblock used in this study revealed a P2VP inner core, surrounded by

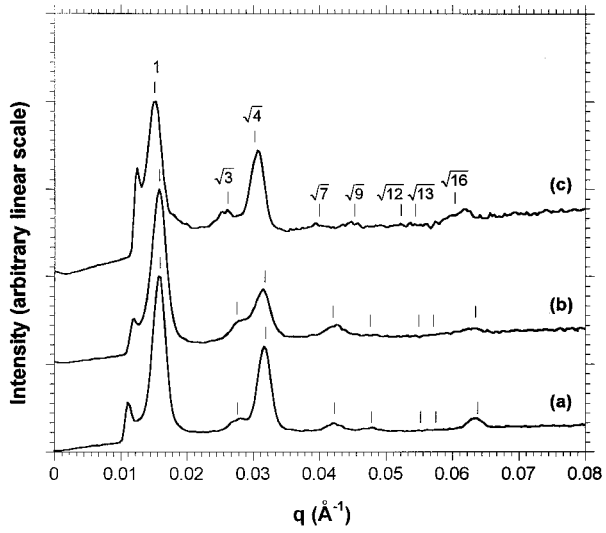

Figure 2. One-dimensional SAXS diffraction signatures of the neat P2VP−PI−PS triblock copolymer (a), PIS/S-1 (b), and PIS/S-2 (c). The domain spacing, *D*, for each sample was calculated using the strongest reflections of those permissible for hexagonal ordering (the first eight are indicated by vertical hash marks above each diffraction signature).

a PI annulus (dark due to OsO_4 staining) in a PS matrix.[12] Both images shown in Figure 1 display nearly axial projections of the P2VP/PI core/annulus arranged in a hexagonal lattice. Macrophase separation in PIS/S-1 and PIS/S-2 was not observed in our TEM characterization of these samples.

A hexagonally packed microstructure is also consistent with the results of a SAXS characterization of these systems shown in Figure 2. The moduli of the first eight permitted reflections corresponding to a hexagonally ordered morphology are indicated by vertical hash marks above the diffraction signatures of the neat P2VP−PI−PS triblock (part a), PIS/S-1 (part b), and PIS/S-2 (part c). The domain spacing, *D*, for each system was obtained by fitting the positions of the strongest observed reflections to those expected for hexagonal symmetry, using *D* as a variational parameter. Any absent peaks (notably, $\sqrt{12}$ and $\sqrt{13}$) are a result of the coincidence of a minimum in the microdomain form factor with a lattice peak. For the neat triblock (part a), $D = 394 \pm 2$ Å (using the 1, $\sqrt{3}$, $\sqrt{4}$, and $\sqrt{16}$ reflections), for PIS/S-1 (part b), $D = 396 \pm 2$ Å (using the 1, $\sqrt{3}$, $\sqrt{4}$, and $\sqrt{7}$ reflections), and for PIS/S-2 (part c), $D = 416 \pm 2$ Å (using the 1, $\sqrt{3}$, $\sqrt{4}$, and $\sqrt{16}$ reflections). We find that the values of the domain spacing obtained for PIS/S-1 and PIS/S-2 via SAXS are consistent with those measured from the micrographs.

Parts a and b of Figure 1 are distinguished by the shape of the PI/PS IMDS. In the image shown in part a, "corners" are observed, indicating a non-CMC PI/PS IMDS. The thickness of the PI annulus exhibits an azimuthal dependence, ranging from a minimum of ∼90 Å to a maximum of ∼110 Å when measured along a ray passing from the center of each domain through the corner of the Wigner−Seitz cell. In part b, the PI/PS IMDS appears to be nearly circular in projection, suggesting that it is of CMC. Here, the PI annulus exhibits a nearly uniform thickness of ∼100 Å. In both cases, the thickness of the PI annulus may be compared to the unperturbed dimensions of anionically polymerized 1,4-PI. For h-PI having an isomer distribution similar to that in the P2VP−PI−PS triblock, $\langle R_0^2 \rangle = 0.596M$,[20] where $\langle R_0^2 \rangle$ is the mean-square unperturbed dimensions and *M* is the molecular weight. Using this relation, the unperturbed dimension of PI blocks having the same molecular weight as those in the P2VP−PI−PS triblock is 88 Å. Therefore, in both cases the PI blocks are stretched from their unperturbed conformations. This results from the tethering of both ends of the PI midblock and the segment−segment repulsive interactions at each IMDS.

The observation of a non-CMC PI/PS IMDS in part a of Figure 1 is a result of the interface assuming the shape of the Wigner−Seitz cell for a hexagonally packed microstructure. This morphological feature is also observed for the neat P2VP−PI−PS triblock copolymer as reported earlier.[12] The strong coupling of the shape of the PI/PS IMDS to the boundary of the Wigner−Seitz cell results from the inclusion of 60% (66% in the case of the neat P2VP−PI−PS system) of the block copolymer (i.e., the P2VP and PI components) in the core of each microdomain.

Our observations of a cylindrical ABC morphology are analogous to observing hexagonally packed A cylinders within a B matrix in a strongly segregated system of AB diblock copolymers in which $f_A = 0.60-0.66$. Such a morphology is not observed, however, since an alternating lamellar or bicontinuous structure which minimizes unfavorable chain distortion is stable at this composition.[1,21] It is well-known that hexagonally packed cylinders are observed in strongly segregated diblock copolymer systems only when the cylinder-forming component is less than about 30%. In the usual case, the outer blocks constituting the majority component possess sufficient elasticity to dampen the azimuthally dependent block deformation imposed by the Wigner−Seitz cell.

In sharp contrast to the concentric morphologies exhibited by the neat P2VP−PI−PS triblock and the blends shown in Figure 1, TEM characterization of a microphase-separated PI−PS−P2VP triblock copolymer system reveals a lamellar structure.[10,11,13] The neat PI−PS−P2VP copolymer is similar in molecular weight and composition to the P2VP−PI−PS copolymer used in this study. The key difference between the two copolymers is that the PI and PS blocks are transposed, leading to different interfacial tensions characteristic of each set of IMDS. This feature of ABC triblock copolymers has been thoroughly discussed in recent studies.[14,22,23] In a theoretical investigation addressing microphase separation in ABC triblock copolymers,[23] a formalism based on the density functional theory of Ohta and Kawasaki[24,25] was used to predict the phase behavior of the neat PI−PS−P2VP and P2VP−PI−PS copolymers. The results were parametrized in terms of the relative interfacial tensions $\sigma_{PI/PS}/\sigma_{PS/P2VP}$ and $\sigma_{P2VP/PI}/\sigma_{PI/PS}$ for the IMDS exhibited by PI−PS−P2VP and P2VP−PI−PS copolymers, respectively. Lamellae were predicted to be stable in the PI−PS−P2VP system when $1/4.3 \leq \sigma_{PI/PS}/\sigma_{PS/P2VP} \leq 4.3$. The concentric microphase observed in the neat P2VP−PI−PS system[12] was predicted when $\sigma_{P2VP/PI}/\sigma_{PI/PS} > 4.3$.

To compare our observations with the theoretical calculation, we calculate $\sigma_{PI/PS}$, $\sigma_{PS/P2VP}$, and $\sigma_{P2VP/PI}$ in the limit of strong segregation.[21,26] Table 3 shows the results of a calculation of the interfacial tension of the various IMDS present in microphase-separated P2VP−

Table 3. Comparison of the Interfacial Tensions for the IMDS Present in Strongly-Segregated P2VP−PI−PS and PI−PS−P2VP Triblock Copolymer Systems

IMDS	χ (120 °C)	$\alpha_\chi{}^c$ (mmol/cm^3)	$\alpha_\delta{}^c$ (mmol/cm^3)	$\sigma_\chi{}^d$ (dyn/cm)	$\sigma_\delta{}^d$ (dyn/cm)
PI/PS	0.09[a]	0.90	1.03	15.6	16.7
PS/P2VP	0.13[b]	1.30	1.03	18.7	16.7
P2VP/PI			4.15		33.4

[a] From ref 27: $\chi(T) = -0.0419 + 38.54/T$ (K) for PI−PS diblocks. [b] From ref 28: $\chi(T) = -0.033 + 63/T$ (K) for P2VP−PS diblocks. [c] Calculated for IMDS A/B using $\alpha_\chi = \chi\rho_0$ and $\alpha_\delta = (RT)^{-1}(\delta_A - \delta_B)^2$. See refs 21 and 26. [d] Calculated from ref 21 using $\sigma/RT = 6^{1/2}\alpha^{1/2}\rho_0{}^{1/2}b$. In footnotes *c* and *d* we assume a constant molar density, $\rho_0 \sim 10$ mmol/cm^3, and statistical segment length, $b \sim 6.5$ Å, for all polymer species.

PI−PS and PI−PS−P2VP triblock copolymers. The interfacial tensions σ_χ and σ_δ are calculated using χ-values and solubility parameters, respectively. Although a calculation based on χ-values is preferred, we are required to consider results based on solubility parameters since we are unaware of a measured χ for a P2VP−PI diblock. We find that σ_χ is close to σ_δ for the PS/PI IMDS. We also observe this for the P2VP/PS IMDS. Therefore, we argue that σ_δ is a reasonable approximation for σ_χ for our purposes. For PI−PS−P2VP, we find that $\sigma_{PI/PS}/\sigma_{PS/P2VP} \sim 0.8-1.0$ lies well within the predicted region of stability for a lamellar microphase. For the P2VP−PI−PS copolymers, $\sigma_{P2VP/PI}/\sigma_{PI/PS} \sim 2.0$, which is less than half of the theoretically predicted lower bound of the experimentally observed concentric cylinder microphase. This discrepancy most likely results from the approximations present in the theoretical development and our rather crude calculation of interfacial tension. It would be an interesting exercise to repeat the calculation utilizing a refined version of the formalism used here.[5] However, it is our view that the value of $\sigma_{P2VP/PI}/\sigma_{PI/PS}$ from such a calculation would not predict that the concentric microstructure was more stable than lamellae.

We note that, in developing their theoretical formalism, the authors did not consider that the PI−PS IMDS present in the concentric morphology was of non-CMC.[23] We expect this simplification will not have a pronounced effect for our system but may become limiting as the PI−PS IMDS moves closer to the boundary of the Wigner−Seitz cell (relatively short PS blocks).[12,29] We also expect that the theoretical development will adequately describe the blends shown in Figure 1, since the small quantity of h-PS added into the matrix phase is insufficient to effect a change in the neat microdomain symmetry.

Having discussed the origin of the concentric cylinder morphologies shown in Figure 1, we now discuss the transition in the PI/PS IMDS from non-CMC (part a) to CMC (part b). We propose that a change in the distribution of the added h-PS as a function of its molecular weight drives the transition in the shape of the PI/PS IMDS. Moreover, the h-PS distribution within the PS matrix also accounts for the variation in the domain spacings calculated from Figure 2.

Parts a and b of Figure 3 are a proposed schematic of the microscopic view of a single Wigner−Seitz cell (its boundary is indicated by dashed gray lines) of the morphologies shown in parts a and b of Figure 1, respectively. In this figure, the relative areas of the P2VP, PI, and PS domains have been derived from the bulk composition ratio of 30:30:40 vol %, respectively, and the assumption of incompressibility. We draw the

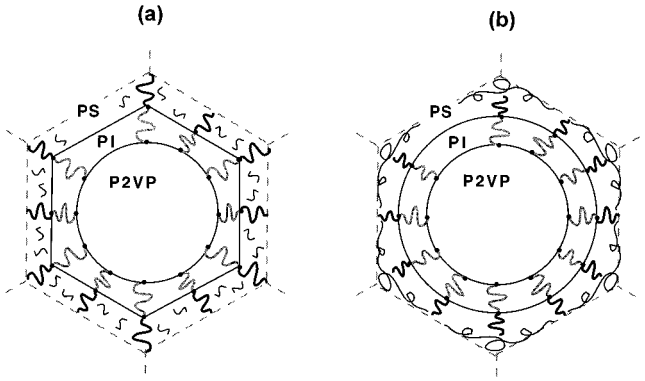

Figure 3. Schematic representations (a and b) of the block copolymer chain conformations in a single microdomain observed in parts a and b of Figure 1, respectively. In each schematic, the boundary of the Wigner−Seitz cell is indicated as dashed gray lines. The PI and PS blocks are shown by thick gray and dark curves, respectively. h-PS is shown by thin dark lines. Note that the polymer chain trajectories are artificially constrained to lie within one Wigner−Seitz cell.

schematics assuming nonoverlapping PS blocks in the corona of the Wigner−Seitz cell. This assumption is not critical to our analysis, and its implication has been discussed previously.[12]

Since the focus of our discussions is centered on the PI and PS blocks of the copolymer and h-PS, we indicate these components in Figure 3 as thick gray, thick dark, and thin dark curves, respectively. As in previous studies, investigating the morphology of blends of h-PS with PS−PI diblock copolymers,[30−38] we also find it illuminating to discuss our model in terms of the ratio of the molecular weight of the added h-PS to that of the PS block in the P2VP−PI−PS copolymer, $r = (M_w)_{h-PS}/(M_w)_{PS}$, for each blend studied.

In part a of Figure 3 (corresponding to PIS/S-1) a nearly uniform distribution of h-PS throughout the matrix phase is proposed. The tethered PS blocks in PIS/S-1 ($r \sim 0.3$) are classified by the so-called "wet brush" regime, defined for systems in which $r \leq 1$.[30−33] In the wet brush regime, the h-PS is fully solubilized within the matrix, maximizing its translational entropy. If present in high-volume fractions, the added h-PS will promote changes in microdomain geometry.[30,31] However, h-PS in PIS/S-1 is present in a sufficiently small quantity, preserving not only the microdomain structure of the neat triblock but also the non-CMC shape of the PI/PS IMDS. This situation also exists for PIS/S blends cast from THF having $r \sim 0.6$ and $r \sim 1.6$. These observations are in line with previous studies suggesting that a transition from the wet brush to the "dry brush" regime occurs when $r > 1$.[34]

The slight decrease in the domain spacing of PIS/S-1 ($D = 394 \pm 2$ Å) relative to its value for the neat triblock ($D = 396 \pm 2$ Å) is also characteristic behavior of the wet brush regime. Although the statistical significance of this difference may be debated, the observed trend has precedence.[33] In a morphological study of blends of a nearly symmetric PS−PI diblock copolymer with h-PS having $r = 0.1-1.4$, the phenomenon of "lamellar contraction" was observed.[33] Specifically, when $r = 0.1$ and the h-PS component comprised 10 wt % of the blend, the lamellar domain spacing decreased by approximately 3% relative to that measured for the neat PS−PI diblock sample.[33] The contraction of the lamellae was rationalized through an increase in the area-per-junction resulting from the PS layer being uniformly

swollen by h-PS.[33] An increase in the area-per-junction increases the spacing between adjacent PI blocks in the neighboring PI lamellae, facilitating a collapse of the PI blocks from their strongly stretched conformations characteristic of the neat PS−PI diblock. The degree of collapse of the PI lamellae was greater than the amount of PS domain swelling, and, consequently, an overall decrease in the lamellar domain spacing was observed.[33] We expect an identical mechanism to be in play in PIS/S-1, since this system is in the wet brush regime and has an r-value and h-PS content to those of the PS−PI/h-PS blend just described. The only complicating factor in our case is the presence of the P2VP core block. However, we do not expect the conformation of the P2VP blocks to be significantly affected by the presence of such a small amount of h-PS in the matrix since the P2VP blocks are one block removed from the PI/PS IMDS, and hence weakly coupled to the small perturbations in junction spacing occurring at that interface.

The physical situation proposed in part b of Figure 3 to account for the "rounding" of the PI/PS IMDS in the PIS/S-2 ($r \sim 3.4$) is characteristic of the dry brush regime.[34−36] In this regime, the h-PS component is nonuniformly distributed in the matrix, tending to segregate from the PS component of the triblock. In our model, we suggest that the relatively high molecular weight h-PS preferentially segregates to the corners of the Wigner−Seitz cells. This phenomenon has the effect of relieving the azimuthally dependent PI block stretching. The PI blocks can thus assume conformations narrowly distributed about an equilibrium value, minimizing the entropic penalty associated with nonuniform deformations.

We note that, although no macrophase separation was observed in PIS/S-2, we observed large domains ($\sim 1\ \mu$m) of pure h-PS in a TEM characterization of a PIS/S blend in which $r \sim 6.7$. Also present in this sample were well-ordered grains of block copolymer material having a morphology identical with that of the neat P2VP−PI−PS triblock sample. We conclude that this phenomenon is consistent with previous observations of PS−PI/h-PS blends deep within the dry brush regime, $r \gg 1$.[34,35] For example, a 40/60 (wt %) blend of a symmetric PS−PI diblock copolymer with h-PS having $r = 11.5$ exhibited "islands" of lamellae (the morphology characteristic of the neat diblock) within a "sea" of h-PS.[35] The investigators also determined that the domain spacing of the lamellae did not vary as a result of forming the blend and concluded that little h-PS was solubilized within the lamellar "islands".[35] Although r was larger and h-PS constituted a greater fraction of the blend in this study when compared to PIS/S-2, we expect that the same physical mechanisms are dictating the microstructure in both systems.

We close with a few remarks concerning further experimentation on the PIS/S blends. In preparing the blends we attempted to double r each time a higher molecular weight h-PS was employed. We noticed the transition in the curvature of the PI/PS IMDS as r jumped from 1.6 to 3.4. Most likely, the transition in curvature occurs when $1.6 < r < 3.4$ for the blend composition studied here. It would be of interest to pinpoint the r-value at the transition point as well as determine its sensitivity to the overall h-PS content in the PIS/S blend.

Our statement regarding the preferential segregation of h-PS to the *corners* of the Wigner−Seitz cell in PIS/S-2 is made with some degree of speculation. h-PS may be distributed more uniformly about the periphery of a Wigner−Seitz cell and still promote rounding of the PI/PS IMDS. An ambitious set of experiments would be to enhance the contrast of h-PS relative to PS in the triblock through deuteration. Characterization of PIS/d-S blends similar to those studied here through SANS may yield information on the distribution of deuterated h-PS within the matrix phase.[39]

Finally, blends of P2VP−PI−PS with either h-P2VP or h-PI may promote morphology transitions not observed here. In such blends, homopolymer would be incorporated into the discontinuous phases, and transitions from the hexagonally packed morphology to other novel morphologies are likely.

4. Conclusions

Our study demonstrates that homopolymer distribution can be inferred from a *visual* study of the cross-sectional shape of the IMDS in microphase-separated block copolymer/homopolymer blends. Moreover, for the microstructure studied here, a small amount of added homopolymer was shown to have a pronounced effect on the microstructure of the PIS/S blends. Most notably, the shape of the PI/PS IMDS was quite sensitive to the molecular weight of h-PS component.

The PIS/S blends characterized in this study exhibited morphological characteristics spanning the wet brush and dry brush regimes. First, the equilibrium nature of the hexagonally packed microstructure having a non-CMC PI/PS IMDS observed in the neat P2VP−PI−PS triblock was established by its insensitivity to the sample preparation protocol. When the triblock was blended with a small amount of h-PS having $r \sim 0.3$ (PIS/S-2), the non-CMC character of the PI/PS IMDS persisted. Also, a slight contraction in the domain spacing in PIS/S-1 was observed. When combined, these observations clearly show that the tethered PS blocks behave as wet brushes, suggesting a nearly uniform distribution of the relatively low molecular weight h-PS throughout the matrix phase.

As the molecular weight of h-PS in the blend is increased, the expected transition from the wet brush to the dry brush regime is finally observed when $r \sim 3.4$ (PIS/S-2). In PIS/S-2 the PI/PS IMDS is of CMC, with an accompanying increase in the domain spacing relative to the neat triblock. These two results indicate that the sample is well within the dry brush regime. Moreover, we propose (but do not explicitly confirm) that the higher molecular weight h-PS in PIS/S-2 segregates to the periphery of the Wigner−Seitz cell, most likely residing at the corners. This phenomenon would promote the relief of the azimuthally dependent PI block deformation and its associated entropic penalty. A reduction of the interfacial enthalpic penalty as a result of forming a CMC IMDS also occurs in this case. We propose that these two factors compensate for the loss in translational entropy of h-PS as a result of its localization.

In PIS/S blends more deeply within the dry brush regime, macrophase separation of h-PS from the microdomains formed by the neat triblocks was observed. Further, the microdomain structure appeared to be nearly identical with that of the neat triblock, again exhibiting the non-CMC IMDS. These observations

suggest that the relatively high molecular weight h-PS was completely ejected from the tethered PS blocks.

Acknowledgment. We thank C. Honeker, D. Hajduk, and S. Gruner for facilitating the SAXS characterization of the materials. We are also grateful to B. Carvalho for several stimulating discussions concerning our results. Finally, we acknowledge NSF under Grant DMR 92-14853 and AFOSR under Grant F49-620-94-1-004 for financial support of this work.

References and Notes

(1) Thomas, E. L.; Lescanec, R. L. *Philos. Trans. R. Soc. London, Ser. A* **1994**, *348*, 149.
(2) Binder, K. *Adv. Polym. Sci.* **1994**, *112*, 183.
(3) Bates, F. S.; Fredrickson, G. H. *Annu. Rev. Phys. Chem.* **1990**, *41*, 525.
(4) Anderson, D. M.; Thomas, E. L. *Macromolecules* **1988**, *21*, 3221.
(5) Matsen, M. W.; Bates, F. S. *J. Chem. Phys.* **1997**, *106*, 2436.
(6) Matsushita, Y.; Chosi, H.; Fujimoto, T.; Kawai, H. *Macromolecules* **1980**, *13*, 1053.
(7) Arai, K.; Kotaka, T.; Kitano, Y.; Yoshimura, K. *Macromolecules* **1980**, *13*, 1670.
(8) Kudose, I.; Kotaka, T. *Macromolecules* **1984**, *17*, 2325.
(9) Shibayama, M.; Hasegawa, H.; Hashimoto, T.; Kawai, H. *Macromolecules* **1982**, *15*, 274.
(10) Mogi, Y.; Kotsuji, H.; Kaneko, Y.; Mori, K.; Matsushita, Y.; Noda, I. *Macromolecules* **1992**, *25*, 5408.
(11) Mogi, Y.; Mori, K.; Matsushita, Y.; Noda, I. *Macromolecules* **1992**, *25*, 5412.
(12) Gido, S. P.; Schwark, D. W.; Thomas, E. L.; Goncalves, M. *Macromolecules* **1993**, *26*, 2636.
(13) Mogi, Y.; Mori, K.; Kotsuji, H.; Matsushita, Y.; Noda, I. *Macromolecules* **1993**, *26*, 5169.
(14) Stadler, R.; Auschra, C.; Beckmann, J.; Krappe, U.; Voigt-Martin, I.; Leibler, L. *Macromolecules* **1995**, *28*, 3080.
(15) Breiner, U.; Krappe, U.; Thomas, E. L.; Stadler, R. *Macromolecules* **1998**, *31*, 135.
(16) Sioula, S.; Hadjichristidis, N.; Thomas, E. L. *Nature* **1998**, submitted.
(17) Morton, M.; Fetters, L. J. *Rubber Chem. Technol.* **1975**, *48*, 359.
(18) Tate, M. W.; Gruner, S. M.; Eikenberry, E. F. *Rev. Sci. Instrum.* **1997**, *68*, 47.
(19) Brandrup, J., Immergut, E. H., Eds. *Polymer Handbook*; Interscience: New York, 1966.
(20) Fetters, L. J.; Lohse, D. J.; Richter, D.; Witten, T. A.; Zirkel, A. *Macromolecules* **1994**, *27*, 4639.
(21) Helfand, E.; Wasserman, Z. R. *Developments in Block Copolymers*; Goodman, I., Ed.; Elsevier: New York, 1982; Vol. 1.
(22) Nakazawa, H.; Ohta, T. *Macromolecules* **1993**, *26*, 5503.
(23) Zheng, W.; Wang, Z.-G. *Macromolecules* **1995**, *28*, 7215.
(24) Ohta, T.; Kawasaki, K. *J. Chem. Phys.* **1986**, *87*, 697.
(25) Ohta, T.; Kawasaki, K. *Macromolecules* **1990**, *23*, 2413.
(26) Helfand, E.; Sapse, A. M. *J. Chem. Phys.* **1975**, *62*, 1327.
(27) Hashimoto, T.; Igichi, Y.; Fetters, L. J. *J. Chem. Phys.* **1988**, *89*, 2463.
(28) Dai, K. H.; Kramer, E. J. *Polymer* **1994**, *35*, 157.
(29) Fredrickson, G. H. *Macromolecules* **1993**, *26*, 4351.
(30) Tanaka, H.; Hasegawa, H.; Hashimoto, T. *Macromolecules* **1991**, *24*, 240.
(31) Winey, K. I.; Thomas, E. L.; Fetters, L. J. *Macromolecules* **1992**, *25*, 2645.
(32) Matsen, M. W. *Macromolecules* **1995**, *28*, 5765.
(33) Winey, K. I.; Thomas, E. L.; Fetters, L. J. *Macromolecules* **1991**, *24*, 6182.
(34) Koizumi, S.; Hasegawa, H.; Hashimoto, T. *Makromol. Chem. Macromol. Symp.* **1992**, *72*, 75.
(35) Koizumi, S.; Hasegawa, H.; Hashimoto, T. *Macromolecules* **1994**, *27*, 6532.
(36) Likhtman, A. E.; Semenov, A. N. *Macromolecules* **1997**, *30*, 7273.
(37) Koizumi, S.; Hasegawa, H.; Hashimoto, T. *Macromolecules* **1994**, *27*, 7893.
(38) Hashimoto, T.; Tanaka, H.; Hasegawa, H. *Macromolecules* **1990**, *23*, 4378.
(39) Turner, D. C.; Gruner, S. M.; Huang, J. S. *Biochemistry* **1992**, *31*, 1356.

MA971426+